

Matthew L. Gorrington · H. R. Naslund

Geochemical reversals within the lower 100 m of the Palisades sill, New Jersey

Received: 11 December 1993 / Accepted: 2 August 1994

Abstract Transects through the lower part of the Palisades sill were made at Fort Lee and Alpine, New Jersey in order to characterize the petrologic signature of previously proposed “reversals” in the normal, tholeiitic differentiation trend. Petrographic and geochemical data include: (1) modal and grain size analyses, (2) bulk rock major and trace element concentrations by DCP-AES, and (3) augite, orthopyroxene, magnetite, and olivine compositions by electron microprobe analysis. Anomalous horizons, defined by increased bulk rock Mg#, Cr, Ni, and Co concentrations and abrupt modal and grain-size changes, occur at 10 m (the well known olivine zone), 27 m, 45 m, and 95 m above the basal contact. Thermal models coupled with estimates of the emplacement rate and total magma volume indicate that the olivine zone (OZ) is an early-stage feature, related to the emplacement of initial magma into the Palisades chamber. Stoke’s Law calculations indicate that the settling velocity of average-sized olivine crystals in a high-titanium, quartz-normative (HTQ) magma is too slow for significant gravity settling to have occurred prior to the solidification of the basal 20 m of the sill. It is suggested that the OZ resulted from the emplacement of a heterogeneous initial magma from a compositionally stratified, sub-Palisades storage chamber located within the upper crust; however, heterogeneity may have been derived directly from the mantle or during rapid ascent. Geochemical models indicate that the OZ contains accumulated olivine that is not in cotectic (or constant)

proportions with the other cumulus phases, suggesting a mechanical sorting process. Magma chamber recharge is proposed to have occurred at the 27 m and 45 m levels, when a slightly more-primitive HTQ magma was injected into the Palisades sill chamber. Zones of elevated Mg# and Cr, 6 to 10 m thick, at these two horizons may indicate the thickness of the hybrid magma formed by the mixing of these two compositions. Geochemical models indicate that the rocks at these levels have accumulated excess orthopyroxene relative to samples from the rest of the sill. Normal faulting in the Fort Lee area at the 95 m level has caused repetition of the stratigraphic section, and hence, the sharp reversal observed at this level.

Introduction

Previous investigations and petrogenetic models

The Palisades sill has a U-Pb radiometric age of 201 ± 1 Ma (Dunning and Hodych 1990) and is located in the northern part of the Newark Basin (Fig. 1A, B) which is the largest of several major Triassic-Jurassic rift basins located in eastern North America. The Palisades sill is a sheet-like, tholeiitic intrusion approximately 300 m thick and at least 80 km in length; however, the sill may be up to 150 km in length (Husch 1990, 1992), extending from southeastern New York to eastern Pennsylvania. The chilled margins of the sill are typical high-Ti, quartz normative (HTQ) basalt commonly found within the eastern North American (ENA) Mesozoic igneous province (Weigand and Ragland 1970). The Palisades sill crystallized a thick (250 m) floor sequence and thin (50 m) roof sequence and displays a well-developed differentiation trend from Mg-rich diabase in the lower sections to incompatible-element enriched, Fe-rich diorites in the upper sections of

M. L. Gorrington (✉) · H. R. Naslund
Department of Geological Sciences,
State University of New York at Binghamton, Binghamton,
NY 13902, USA

¹ Current address:
Department of Geological Sciences, Cornell University,
Ithaca, NY 14853, USA

Editorial responsibility: T. L. Grove

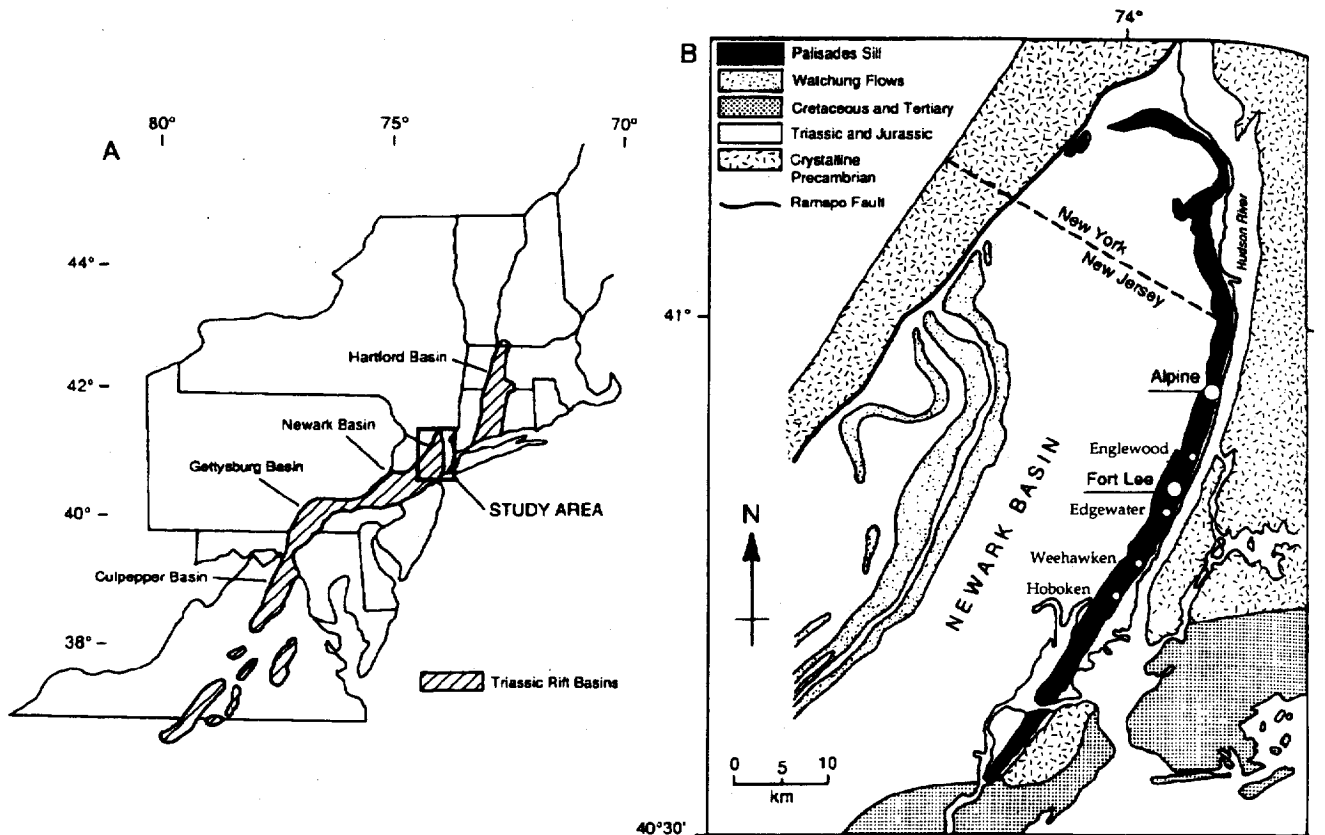


Fig. 1A The general location of Triassic/Jurassic rift basins in the eastern United States, modified from Husch (1990). B Geologic sketch map of the northern Newark Basin, modified from Walker (1969). Samples from the lower part of the Palisades sill were obtained from Fort Lee and Alpine, New Jersey (large open circles); other important localities are also shown (small open circles)

the sill (F. Walker 1940; K. Walker 1969; Shirley 1987). For a more detailed description of the general structural and geochemical features of the sill, the reader is referred to Walker (1969).

Early investigations by Darton (1890), Lewis (1907, 1908), and Walker (1940) established the initial structural and petrologic framework from which the original interpretation of magmatic differentiation by gravity settling of olivine crystals was founded. Hess (1956) was the first to challenge seriously the classic model of gravity settling by proposing an in-situ fractionation model coupled with magmatic convection. Since these early investigations, several modern petrologic studies have been undertaken (Walker 1969; Shirley 1987; Husch 1990, 1992; Gorrington and Naslund 1991a; Steiner et al. 1992) to constrain the petrogenesis of the Palisades sill. These investigations have proposed a variety of differentiation models which generally include complex variations on crystal sorting and/or multiple intrusion mechanisms. Walker (1969) cited evidence from several localities along the length of the sill that were not consistent with crystal settling and suggested that

the olivine zone (OZ) represented a second magma injection. Shirley (1987) collected a geochemical traverse through the Palisades sill at Fort Lee, New Jersey, and on the basis of reversals in bulk rock Mg#, Cr, Ni, and Co, at the 10 m, 35 m, and 95 m stratigraphic levels proposed that there may have been four magma injections. Husch (1990) cites evidence for lateral differentiation processes in the Palisades sill and other similar intrusions in west-central New Jersey due to periodic injections of primitive magma. More recently, Steiner et al. (1992) has suggested that a single-model approach to differentiation in the Palisades sill cannot adequately explain the observed petrologic features of the sill and has proposed the Cumulus-Transport-Deposition (C-T-D) Model.

The OZ of the Palisades sill has received considerable attention recently (Shirley 1987; Husch 1990; Gorrington and Naslund 1991b) since Walker (1969) interpreted the OZ as the result of a second magmatic injection followed by accumulation of olivine near the base by gravity settling. Walker (1969) suggested that the second injection was much larger and more evolved than the initial injection. Walker's interpretations were based primarily on the following observations: (1) the OZ is considerably thinner and contains more Fe-rich olivine than expected when compared to the abundance (1–3%) and composition (Fo_{80}) of olivine in the chilled margin, (2) the OZ is located 10–15 m above the basal contact, and (3) an internally chilled contact and

associated flow banding are present immediately below the OZ at Kings Bluff, NJ. Shirley (1987) and Husch (1990) also interpreted the OZ as a second magma injection; however, gravity settling was largely discounted in their models based on physical and petrologic arguments. Steiner et al. (1992) invoked the C-T-D Model, in which the OZ is an early accumulation of olivine owing to internal processes of crystal sorting and sedimentation, and is neither a product of in-situ gravity settling nor externally-derived multiple injections.

In this study, we present detailed petrologic data combined with quantitative calculations of critical magmatic processes to constrain and evaluate previous models advanced by Walker (1969), Shirley (1987), and Husch (1990). The evidence suggests that the OZ is formed at an early stage, most likely during the initial emplacement process. Other anomalous horizons, above the OZ, can be modeled as discrete magma injections or as the result of normal faulting. The emplacement-recharge model introduced here is similar in some respects to models proposed by Shirley (1987), Husch (1990) and the C-T-D model of Steiner et al. (1992). Fluid dynamical models of Komar (1972), Huppert and Sparks (1980), and Kerr and Tait (1985) are also incorporated into the emplacement-recharge model.

Magma chamber recharge phenomena

The emplacement of magma into a chamber can involve both open- and closed-system phenomena. Magma chambers can fill with liquid during a single emplacement event without subsequent additions or subtractions of magma, and in fact, many Mesozoic tholeiitic sheets within the ENA magmatic province are consistent with essentially closed-system differentiation derived from a single emplacement event (Smith et al. 1975; Froelich and Gottfried 1988). Alternatively, magma chambers can experience periodic influxes of liquid during the solidification process, and these influxes are termed "magma chamber recharge" (equivalent to multiple injection or magma pulse). The geochemical signature of magma chamber recharge in ENA tholeiitic sheets can be characterized by reversals in the normal differentiation trend due to the injection of more-primitive ENA magmas (Shirley 1987; Husch 1990, 1992). Early crystallizing assemblages of mafic liquidus phases such as olivine, clinopyroxene, and orthopyroxene are expected to deplete ENA magmas in MgO and compatible trace elements (i.e. Cr, Ni, Co, and Sc). Reversals in the differentiation trend are usually defined by anomalously abundant compatible elements in whole-rock samples and in cumulus mafic phases (Irvine 1980). Depending on the compositional contrast between the injected and resident magmas, magma chamber recharge can cause geochemical rever-

sals with or without the association of modal discontinuities (Irvine 1980).

Petrology and geochemistry

Sampling and analytical techniques

The data set presented here consists of 150 samples collected from natural and man-made outcrops at Fort Lee and Alpine, New Jersey. These samples form two, composite sections of the lower 105 m (Fort Lee) and the lower 24 m (Alpine) of the Palisades sill, and were collected at stratigraphic intervals of 0.5 to 2 m. A strike of N30E and a dip of 11° NW, was used to correct all stratigraphic heights for horizontal offsets in sampling traverses. Measurements by tape measure and plane table surveying allowed for precise determinations of relative stratigraphic height (± 10 –20 cm). The accuracy of absolute stratigraphic height measurements relative to the basal contact is probably within ± 1 –2 m. Standard petrographic techniques were used to obtain modal and grain size data. Whole-rock analyses for both major and trace elements were obtained by direct current plasma atomic emission spectroscopy (DCP-AES), similar to techniques described by Feigenson and Carr (1985). Ferrous iron was determined by the colorimetric, wet-chemical technique of Wilson (1960). Mineral compositions were determined by standard electron microprobe techniques. The reader is referred to Gorring (1992) for complete details of various sampling and analytical techniques.

Petrography

The mineralogy of the lower 100 m of the Palisades sill is dominated by plagioclase and augite with minor amounts of accessory minerals such as orthopyroxene (or inverted pigeonite), olivine, pigeonite, quartz/alkali-feldspar intergrowths, quartz, ilmenite, magnetite, biotite, and apatite, in order of abundance. All samples have varying degrees of deuteric alteration, usually identified by turbid patches of sericite and uraltite(?) replacing plagioclase and augite, respectively (Walker 1969). The dominant texture is subophitically intergrown augite and plagioclase; however, the texture within the central part of the OZ is strongly poikilitic, with large plagioclase and orthopyroxene oikocrysts enclosing smaller olivine chadocrysts. Modal variations within the lower 100 m of the Palisades sill at Fort Lee are shown in Fig. 2. In general, from the chilled margin to the 20 m level the abundance of plagioclase and augite decreases and the abundance of orthopyroxene increases corresponding with an increase in modal olivine. Above the OZ, between the 20 m and 100 m levels, the modal abundance of plagioclase increases, the abundance of augite remains relatively constant, and the abundance of orthopyroxene decreases. Grain-size measurements of plagioclase and augite from Fort Lee are shown in Fig. 3. The trend for both phases is the expected gradual increase in grain size away from the chilled margin. Larger grain sizes for both phases are evident at the 15 m level, reflecting the change from subophitic to poikilitic texture within the OZ. A sharp decrease in the grain size of augite and plagioclase occurs at approximately the 50 m level, in contrast to earlier reported increases in grain size (Walker 1969; Shirley 1987).

Detailed petrography of the OZ

The petrography of the OZ was investigated in detail at both Fort Lee and Alpine. The modal abundance of olivine versus stratigraphic height is shown in Fig. 4A. The location of the OZ is defined by large increases in modal olivine, from essentially 0% above and below the horizon, to a maximum of 28% within the central part of

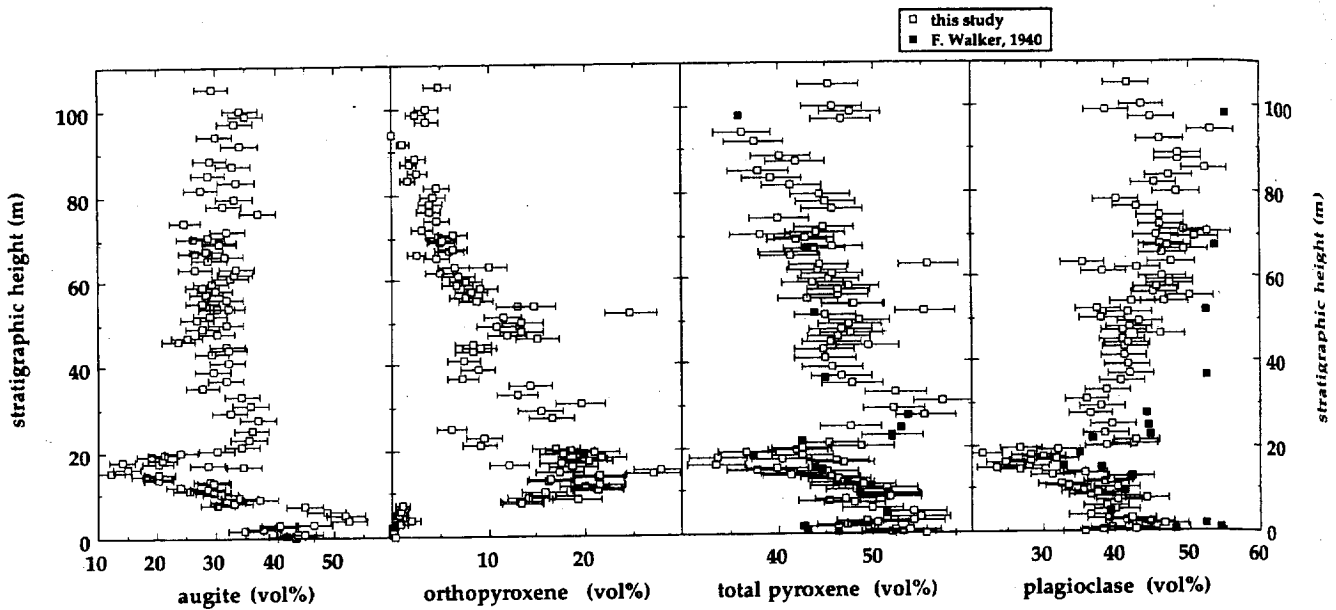


Fig. 2 Modal abundance (vol. %) versus stratigraphic height (m) for augite, orthopyroxene, total pyroxene, and plagioclase from the Fort Lee section. Data from this study (*open squares*) and Walker (1940) (*filled squares*). Error bars represent the 95% confidence interval (2σ) calculated by the method of Van Der Plas and Tobi (1965)

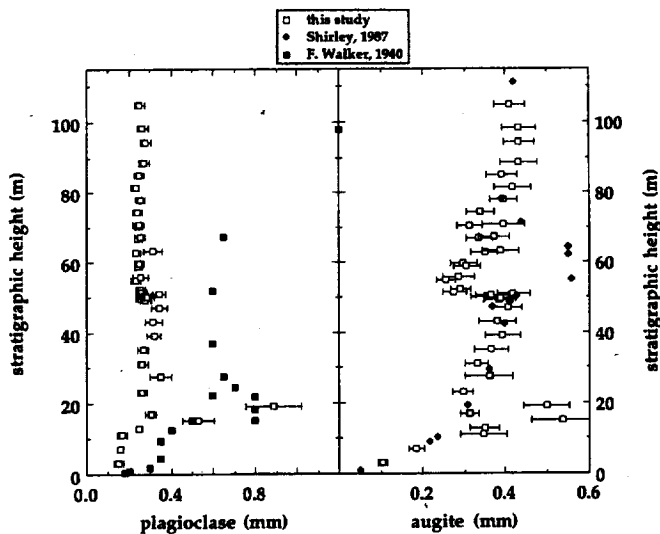


Fig. 3 Average grain size (mm) versus stratigraphic height (m) for plagioclase and augite from the Fort Lee section. Data from this study (*open squares*), Walker (1940) (*filled squares*), and Shirley (1987) (*filled diamonds*). Error bars represent the 95% confidence interval (2σ) based on 200 measurements per sample. Note: data from Shirley (1987) represent average grain size of all phases.

the horizon. The OZ occurs at about 10 m above the basal contact at both Fort Lee and Alpine; however, it is considerably thicker at Fort Lee (10–12 m) than it is at Alpine (6–7 m). Subophitic texture is generally preserved in the lower parts of the OZ, where olivine

occurs as relatively large (0.6–0.8 mm diameter), partially resorbed, anhedral grains. In contrast, the central and upper parts of the OZ are characterized by a well-developed poikilitic texture defined by abundant, small (0.1–0.3 mm diameter), euhedral olivine grains enclosed in plagioclase and orthopyroxene. Except for a few embayed and altered grains in a sample from the 27 m level at Fort Lee (also noted by Walker 1940), olivine was not identified in any samples above the OZ at either Fort Lee or Alpine. At Fort Lee, modal olivine gradually increases from 1% to 6% between 5 and 11 m; however, this trend is complicated by local minima at 10 m and 12 m. Above the 12 m level, the modal abundance of olivine rapidly increases to 28% at 18 m. In contrast, the modal abundance of olivine in the Alpine section is characterized by relatively constant values of 1–2% between 5 and 11 m, followed by an abrupt increase to a maximum of 17% at 12.5 m. At both Fort Lee and Alpine, the modal abundance of olivine remains relatively high (10–25%) through the central and upper parts of the OZ; however, a complex internal structure is defined by two maxima, separated by diabase with 3–5% olivine. Modal olivine abruptly decreases to 0% at the 20 m and 17 m levels at Fort Lee and Alpine, respectively. The modal abundance of olivine versus stratigraphic height from four other sections through the OZ are shown in Fig. 4B for comparison to the Fort Lee and Alpine sections.

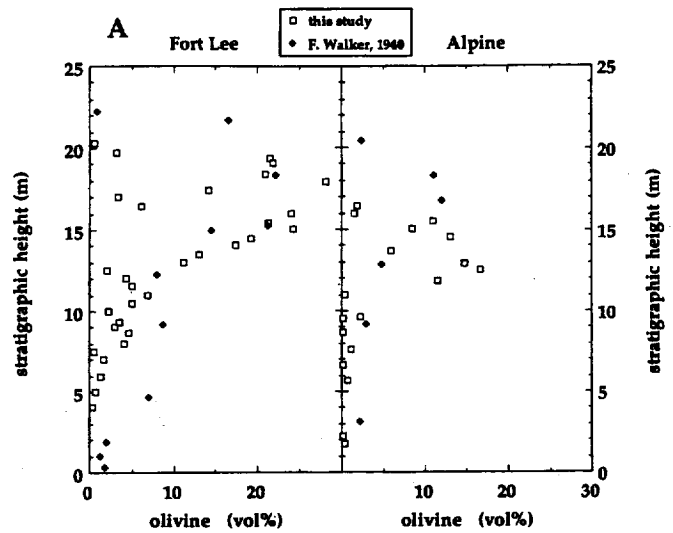
Whole-rock chemistry

Representative whole-rock analyses from Fort Lee, New Jersey are presented in Tables 1 and 2; a more complete data set is available from the authors or can be found in Gorrington (1992). The analyses reported here are similar to previously reported whole-rock data for this part of the sill (Walker 1940; Walker 1969; Shirley 1987). In this study, we have focused on the whole-rock Mg# and Cr, Ni, and Co as these elements are sensitive to the open-system processes discussed earlier (see Table 1 for Mg# definition). The Mg#, Cr, Ni, and Co data from this study and from Walker (1980) and Shirley (1987) for the Fort Lee section are plotted versus stratigraphic height in Fig. 5. Overall, there is good

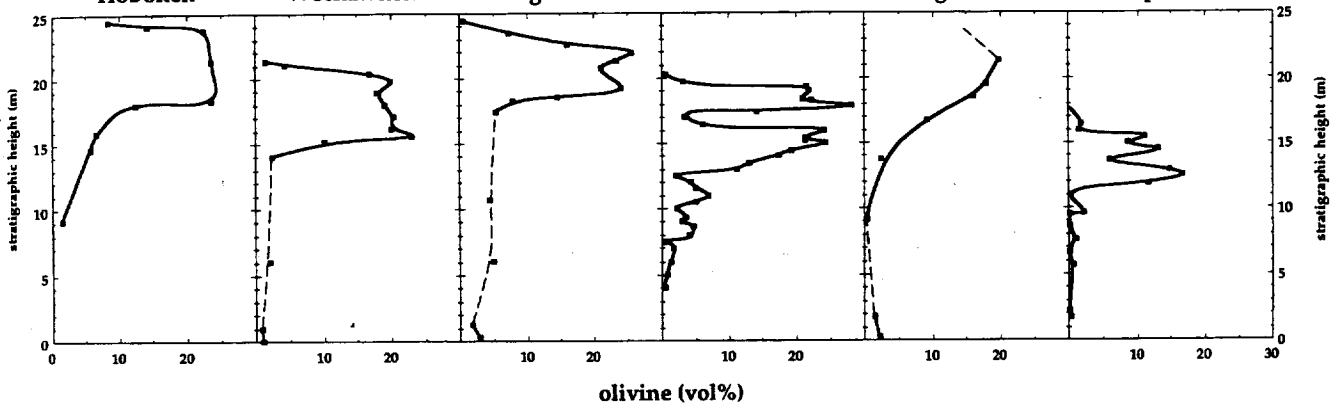
Fig. 4A Modal abundance of olivine (vol.%) versus stratigraphic height (m) from the Fort Lee and Alpine sections. Data from this study (open squares) and Walker (1940) (filled diamonds). B Modal abundance of olivine (vol. %) versus stratigraphic height (m) through the OZ from six locations, representing an along strike profile from Hoboken (south) to Alpine (north). Data (filled squares) from Walker (1940), except for the Fort Lee and Alpine sections which are from this study (Fig. 4A)

100
30
50
40
20

stratigraphic height (m)



B Hoboken Weehawken Edgewater Fort Lee Englewood Alpine



agreement between data presented here and that from previous works; however, the Cr data of Shirley (1987) seem to be systematically higher than ours, probably due to different analytical methods. Between the chilled margin and the OZ (0–10 m) the Mg#, Cr, Ni, and Co all gradually increase. The OZ displays a unique geochemical signature, where higher values of Mg#, Ni, and Co, and lower values of Cr, occur between 10–20 m, details of which are discussed in the following sections. Above the OZ (> 21 m), the normal differentiation trend (decreasing Mg# and Cr with relatively constant Ni and Co) is punctuated by anomalous horizons or “reversals” that are defined by higher values of Mg#, Cr, and Ni at the 27 m, 45 m, and 95 m stratigraphic levels. The anomalous horizon at 27 m is defined by distinctly higher values of Mg#, Cr, and Ni over the interval from 27 m to 33 m before a normal differentiation trend is reestablished. The reversal at the 45 m level is defined primarily by higher Cr, but slight increases in Mg# and Ni also occur. The Cr content remains relatively high between the 45 and 55 m levels,

before sharply decreasing just above the 55 m level. An extremely sharp reversal in the normal differentiation trend occurs at the 95 m level, with significant increases in Mg# and Cr across an apparent stratigraphic interval of less than 3 m. The anomalous horizons defined here broadly correspond to those identified by Shirley (1987), with the exception of the horizon at 27 m, which had not been previously identified. In general, Shirley's data indicate stronger reversals in Mg#, Cr, Ni, and Co than do our data.

Whole-rock chemistry of the OZ

The Mg#, Cr, Ni, and Co data of the OZ for both the Fort Lee and Alpine sections are plotted versus stratigraphic height in Fig. 6. At Fort Lee, variations in Mg# are distinctly gradational from the chilled margin up to the central part of the OZ (15 m); whereas Ni, Co, and Cr variations are gradational between 5 m and

sorted,
the OZ
ned by
grains
a few
level
ntified
ne. At
o 6%
y local
modal
ntrast,
terized
llowed
t both
ains
parts
ed by
olivine
rt Lee
versus
OZ are
Alpine

Lee,
more
r can
here
a for
Shirley
rock
ensi-
:(see
d Co
Shir-
rsus
good

Table 1 Major element composition of Palisades diabase; Fort Lee, New Jersey^a

| Sample | Ht (m) ^b | SiO ₂ | TiO ₂ | Al ₂ O ₃ | Fe ₂ O ₃ ^c | FeO ^c | MnO | MgO | CaO | Na ₂ O | K ₂ O | P ₂ O ₅ | Total | Mg# ^d |
|--------------------|---------------------|------------------|------------------|--------------------------------|---|------------------|------|-------|-------|-------------------|------------------|-------------------------------|--------|------------------|
| A-0.1 ^e | -0.1 | 68.78 | 0.30 | 14.44 | 0.80 | 0.97 | 0.07 | 3.00 | 1.60 | 7.51 | 0.46 | 0.09 | 98.02 | |
| A0.2 | 0.2 | 52.77 | 1.15 | 14.22 | 2.25 | 8.06 | 0.18 | 7.44 | 10.51 | 2.03 | 0.77 | 0.14 | 99.52 | 0.568 |
| A1.0 | 1.0 | 52.30 | 1.16 | 14.31 | 2.24 | 8.11 | 0.18 | 7.31 | 10.28 | 2.11 | 0.91 | 0.15 | 99.06 | 0.563 |
| A3.0 | 3.0 | 52.63 | 1.11 | 14.02 | 2.10 | 8.25 | 0.18 | 7.99 | 10.37 | 2.02 | 0.82 | 0.14 | 99.63 | 0.584 |
| B5 | 5.0 | 51.16 | 0.97 | 12.49 | 1.66 | 8.02 | 0.17 | 9.71 | 10.21 | 1.81 | 0.64 | 0.12 | 96.96 | 0.645 |
| B7 | 7.0 | 50.84 | 1.00 | 13.19 | 1.81 | 8.16 | 0.17 | 9.55 | 10.41 | 1.88 | 0.68 | 0.09 | 97.78 | 0.635 |
| B9 | 9.0 | 50.38 | 0.87 | 10.87 | 1.53 | 8.84 | 0.18 | 13.05 | 9.76 | 1.52 | 0.46 | 0.11 | 97.57 | 0.695 |
| B11 | 11.0 | 49.75 | 0.89 | 11.33 | 2.63 | 8.29 | 0.18 | 13.78 | 9.39 | 1.52 | 0.66 | 0.07 | 98.49 | 0.697 |
| B13 | 13.0 | 49.08 | 0.81 | 10.41 | 1.61 | 9.13 | 0.18 | 14.83 | 8.68 | 1.36 | 0.41 | 0.11 | 96.61 | 0.714 |
| B14 | 14.0 | 47.54 | 0.76 | 10.04 | 1.77 | 10.22 | 0.19 | 17.41 | 7.20 | 1.26 | 0.43 | 0.09 | 96.91 | 0.724 |
| B15 | 15.0 | 47.97 | 0.75 | 8.92 | 2.48 | 11.01 | 0.21 | 20.37 | 7.03 | 1.15 | 0.39 | 0.06 | 100.34 | 0.733 |
| B16 | 15.9 | 47.38 | 0.72 | 9.09 | 2.64 | 10.88 | 0.21 | 18.81 | 6.77 | 1.06 | 0.52 | 0.09 | 98.17 | 0.717 |
| B17 | 16.9 | 50.65 | 1.02 | 13.15 | 2.70 | 7.58 | 0.17 | 10.31 | 10.07 | 1.85 | 0.81 | 0.11 | 98.42 | 0.647 |
| B18 | 17.9 | 46.61 | 0.66 | 9.06 | 2.61 | 11.27 | 0.21 | 18.19 | 6.92 | 1.04 | 0.41 | 0.08 | 97.06 | 0.704 |
| B19 | 19.0 | 47.66 | 0.72 | 8.64 | 1.74 | 12.00 | 0.21 | 18.55 | 7.33 | 1.14 | 0.34 | 0.05 | 98.38 | 0.709 |
| B20 | 19.8 | 50.19 | 0.87 | 11.52 | 2.35 | 9.41 | 0.19 | 12.31 | 9.51 | 1.55 | 0.48 | 0.10 | 98.48 | 0.656 |
| B21 | 21.0 | 52.03 | 0.91 | 13.02 | 1.59 | 7.97 | 0.17 | 9.05 | 10.03 | 1.87 | 0.71 | 0.11 | 97.46 | 0.632 |
| B22 | 21.7 | 52.21 | 0.87 | 12.55 | 1.69 | 8.36 | 0.18 | 9.73 | 10.52 | 1.74 | 0.72 | 0.10 | 98.67 | 0.637 |
| B23 | 23.0 | 52.00 | 0.91 | 12.43 | 1.88 | 8.32 | 0.18 | 10.12 | 10.51 | 1.73 | 0.68 | 0.07 | 98.83 | 0.643 |
| B27 | 27.3 | 52.17 | 0.89 | 11.37 | 2.00 | 8.32 | 0.18 | 11.86 | 10.21 | 1.63 | 0.66 | 0.07 | 99.36 | 0.676 |
| B31 | 31.0 | 51.99 | 0.85 | 11.62 | 1.55 | 8.24 | 0.17 | 11.30 | 10.09 | 1.61 | 0.54 | 0.06 | 98.02 | 0.676 |
| B35 | 35.0 | 52.87 | 0.85 | 12.72 | 1.93 | 7.67 | 0.17 | 9.83 | 10.68 | 1.78 | 0.53 | 0.05 | 99.08 | 0.651 |
| B39 | 39.0 | 53.08 | 0.90 | 12.75 | 2.52 | 7.23 | 0.18 | 9.74 | 10.63 | 1.81 | 0.61 | 0.07 | 99.52 | 0.646 |
| B43 | 43.0 | 52.91 | 0.86 | 12.88 | 1.79 | 7.69 | 0.17 | 9.77 | 10.24 | 1.85 | 0.65 | 0.08 | 98.89 | 0.652 |
| B47 | 47.0 | 53.79 | 0.91 | 12.59 | 1.86 | 7.96 | 0.18 | 10.08 | 10.40 | 1.81 | 0.52 | 0.07 | 100.17 | 0.651 |
| C50 | 50.0 | 53.35 | 0.79 | 11.24 | 1.08 | 8.63 | 0.18 | 11.50 | 9.06 | 1.65 | 0.43 | 0.11 | 98.02 | 0.681 |
| C52 | 52.0 | 53.08 | 0.76 | 12.19 | 1.54 | 8.01 | 0.18 | 11.19 | 10.41 | 1.55 | 0.44 | 0.03 | 99.38 | 0.680 |
| B55 | 55.0 | 52.80 | 0.81 | 14.89 | 1.88 | 6.75 | 0.16 | 8.59 | 11.24 | 1.85 | 0.58 | 0.05 | 99.60 | 0.644 |
| C58 | 57.8 | 52.71 | 0.85 | 13.78 | 1.86 | 7.19 | 0.16 | 9.02 | 11.00 | 1.88 | 0.47 | 0.11 | 99.03 | 0.645 |
| C60 | 59.6 | 52.70 | 0.90 | 13.59 | 1.49 | 7.66 | 0.16 | 9.11 | 11.10 | 1.82 | 0.53 | 0.09 | 99.15 | 0.643 |
| B63 | 63.0 | 52.55 | 0.90 | 14.01 | 1.77 | 7.64 | 0.17 | 8.77 | 11.38 | 1.86 | 0.52 | 0.06 | 99.63 | 0.629 |
| B67 | 67.0 | 52.18 | 0.89 | 14.28 | 1.57 | 7.65 | 0.17 | 8.65 | 11.16 | 1.90 | 0.55 | 0.07 | 99.07 | 0.630 |
| B70 | 70.2 | 52.03 | 0.91 | 14.12 | 1.98 | 7.44 | 0.16 | 8.54 | 11.28 | 1.88 | 0.54 | 0.07 | 98.95 | 0.623 |
| C74 | 74.1 | 52.25 | 0.83 | 14.81 | 1.92 | 6.95 | 0.16 | 8.40 | 11.20 | 2.04 | 0.61 | 0.09 | 99.26 | 0.633 |
| C78 | 77.8 | 52.52 | 0.87 | 14.73 | 1.94 | 7.29 | 0.16 | 8.25 | 11.24 | 2.05 | 0.61 | 0.07 | 99.73 | 0.619 |
| C83 | 83.3 | 52.43 | 0.84 | 15.84 | 1.40 | 7.02 | 0.15 | 7.24 | 10.48 | 2.29 | 0.69 | 0.08 | 98.46 | 0.609 |
| C89 | 88.6 | 52.33 | 0.89 | 14.56 | 1.78 | 7.62 | 0.17 | 7.71 | 11.08 | 2.03 | 0.58 | 0.04 | 98.79 | 0.598 |
| C94 | 94.1 | 52.29 | 0.98 | 14.58 | 2.27 | 7.91 | 0.17 | 7.63 | 11.18 | 2.18 | 0.44 | 0.07 | 99.70 | 0.577 |
| C98 | 98.4 | 52.43 | 0.87 | 13.77 | 1.65 | 7.66 | 0.17 | 9.06 | 10.73 | 2.02 | 0.64 | 0.06 | 99.06 | 0.638 |
| C105 | 104.9 | 52.46 | 0.84 | 13.64 | 1.68 | 7.77 | 0.18 | 8.92 | 11.00 | 1.94 | 0.69 | 0.06 | 99.18 | 0.631 |

^a Major element compositions (weight%) determined by direct current plasma atomic emission spectroscopy (DCP-AES) at SUNY-Binghamton, New York

Major element precision and accuracy based on duplicate analyses of USGS standard BHVO-1 precision is $\pm 2\%$ for K₂O and P₂O₅ for all other oxides precision is $< \pm 1\%$; accuracy is $\pm 2-3\%$ for Al₂O₃, K₂O, P₂O₅; for all other oxides accuracy is $\pm 1\%$

^b Ht (m) = stratigraphic height above the basal contact of the sill in meters

^c FeO determined by wet chemical techniques; Fe₂O₃ = total Fe as Fe₂O₃ - (1.112*FeO)

^d Mg# = (MgO/40.3)/[(MgO/40.3) + ((0.9*Fe₂O₃) + FeO)/71.8]

^e country rock below sill

12 m, and then change abruptly above the 12 m level. Whole-rock trends at Alpine are broadly similar to those observed at Fort Lee, but compositional changes are distinctly more abrupt near the lower contact of the OZ (Fig. 6). Complex internal structure of the OZ at Fort Lee is defined by two maxima in values of Mg#, Ni, and Co, and minima in values of Cr that occur at the 15 m and 19 m levels. At Alpine, similar maxima in the whole-rock Mg#, Ni, and Co, and minima in Cr, occur at the 12.5 m and 15 m levels. The upper contact of the olivine horizon at both localities is marked by a sharp decrease in whole-rock Mg#, Ni, and Co, and

an increase in Cr, over a stratigraphic interval of less than 2 m.

Mineral chemistry

Electron microprobe analyses of augite, orthopyroxene, and magnetite from the lower 60 m of the Fort Lee section were obtained to document any systematic trends in mineral composition and are summarized here. Within the OZ, both augite and orthopyroxene are relatively homogeneous with respect to

Table 2 Trace element composition of Palisades diabase; Fort Lee, New Jersey^a

| Mg # ^d | Sample | Ht (m) ^b | Ba | Co | Cr | Cu | Ni | Sc | Sr | V | Zn | Zr |
|-------------------|--------------------|---------------------|-----|----|-----|-----|-----|------|-----|-----|----------------|-----|
| | A-0.1 ^d | -0.1 | 47 | 21 | 9 | 28 | 9 | 5.1 | 32 | 33 | - ^c | 355 |
| .568 | A0.2 | 0.2 | 189 | 55 | 269 | 114 | 85 | 38.5 | 189 | 268 | - | 96 |
| .563 | A1.0 | 1.0 | 204 | 54 | 246 | 118 | 80 | 38.6 | 206 | 269 | - | 99 |
| .584 | A3.0 | 3.0 | 190 | 64 | 338 | 116 | 96 | 40.4 | 203 | 271 | - | 100 |
| .645 | B5 | 5.0 | 125 | 52 | 725 | 95 | 132 | 42.6 | 167 | 257 | 81 | 102 |
| .635 | B7 | 7.0 | 166 | 53 | 521 | 102 | 136 | 40.4 | 212 | 263 | 78 | 134 |
| .695 | B9 | 9.0 | 116 | 68 | 854 | 87 | 222 | 45.8 | 150 | 247 | 86 | 105 |
| .697 | B11 | 11.0 | 156 | 63 | 636 | 84 | 255 | 41.2 | 189 | 232 | 74 | 131 |
| .714 | B13 | 13.0 | 114 | 74 | 650 | 86 | 287 | 41.3 | 143 | 226 | 88 | 97 |
| .724 | B14 | 14.0 | 137 | 89 | 343 | 80 | 403 | 39.7 | 129 | 217 | - | 110 |
| .733 | B15 | 15.0 | 144 | 92 | 313 | 77 | 499 | 35.2 | 152 | 197 | 88 | 130 |
| .717 | B16 | 15.9 | 143 | 98 | 307 | 68 | 471 | 41.8 | 122 | 207 | - | 116 |
| .647 | B17 | 16.9 | 194 | 63 | 606 | 98 | 178 | 44.3 | 186 | 274 | - | 123 |
| .704 | B18 | 17.9 | 122 | 94 | 303 | 76 | 444 | 39.4 | 111 | 190 | - | 105 |
| .709 | B19 | 19.0 | 136 | 93 | 426 | 91 | 480 | 37.5 | 149 | 190 | 101 | 131 |
| .656 | B20 | 19.8 | 153 | 75 | 622 | 87 | 255 | 47.2 | 157 | 252 | - | 130 |
| .632 | B21 | 21.0 | 139 | 53 | 659 | 94 | 130 | 42.5 | 171 | 256 | 83 | 100 |
| .637 | B22 | 21.7 | 170 | 63 | 739 | 83 | 149 | 51.8 | 177 | 266 | - | 120 |
| .643 | B23 | 23.0 | 162 | 55 | 720 | 90 | 162 | 42.5 | 214 | 260 | 78 | 123 |
| .676 | B27 | 27.3 | 184 | 60 | 817 | 85 | 204 | 45.5 | 185 | 258 | 80 | 126 |
| .676 | B31 | 31.0 | 141 | 58 | 705 | 77 | 177 | 41.1 | 185 | 252 | 73 | 110 |
| .651 | B35 | 35.0 | 147 | 54 | 573 | 84 | 126 | 43.7 | 198 | 260 | 73 | 118 |
| .646 | B39 | 39.0 | 171 | 52 | 527 | 82 | 114 | 44.6 | 205 | 237 | 80 | 115 |
| .652 | B43 | 43.0 | 178 | 49 | 533 | 81 | 114 | 42.9 | 203 | 241 | 78 | 109 |
| .651 | B47 | 47.0 | 146 | 54 | 579 | 86 | 127 | 40.6 | 194 | 253 | 79 | 107 |
| .681 | C50 | 50.0 | 129 | 55 | 693 | 81 | 131 | 46.3 | 148 | 239 | 78 | 98 |
| .680 | C52 | 52.0 | 128 | 56 | 719 | 74 | 139 | 45.4 | 193 | 254 | 75 | 103 |
| .644 | B55 | 55.0 | 161 | 49 | 514 | 81 | 111 | 38.4 | 223 | 256 | 69 | 106 |
| .645 | C58 | 57.8 | 121 | 53 | 541 | 84 | 109 | 43.8 | 178 | 260 | 73 | 95 |
| .643 | C60 | 59.6 | 122 | 52 | 544 | 83 | 111 | 44.0 | 172 | 264 | 72 | 99 |
| .629 | B63 | 63.0 | 141 | 53 | 481 | 100 | 121 | 39.1 | 207 | 286 | 76 | 112 |
| .630 | B67 | 67.0 | 155 | 51 | 435 | 92 | 113 | 41.6 | 216 | 272 | 76 | 114 |
| .623 | B70 | 70.2 | 155 | 47 | 396 | 89 | 104 | 41.5 | 212 | 262 | 73 | 111 |
| .633 | C74 | 74.1 | 162 | 45 | 382 | 72 | 99 | 38.9 | 228 | 247 | 69 | 94 |
| .619 | C78 | 77.8 | 163 | 50 | 370 | 90 | 106 | 39.1 | 221 | 269 | 75 | 107 |
| .609 | C83 | 83.3 | 151 | 46 | 279 | 84 | 83 | 35.6 | 203 | 234 | 68 | 92 |
| .598 | C89 | 88.6 | 165 | 48 | 256 | 91 | 96 | 39.4 | 225 | 254 | 73 | 125 |
| .577 | C94 | 94.1 | 132 | 54 | 204 | 101 | 96 | 40.9 | 228 | 289 | 80 | 134 |
| .638 | C98 | 98.4 | 163 | 51 | 412 | 87 | 115 | 44.5 | 219 | 269 | 73 | 137 |
| .631 | C105 | 104.9 | 186 | 53 | 396 | 85 | 118 | 44.5 | 210 | 275 | 75 | 124 |

SUNY-

^a Trace element compositions (ppm) determined by direct current plasma atomic emission spectroscopy (DCP-AES) at SUNY-Binghamton, New York

^b Trace element precision and accuracy based on duplicate analyses of USGS standard BHVO-1 precision is $\pm 2-4\%$ for Ba and Co; for all other elements precision is $< \pm 2\%$; accuracy is $\pm 2-4\%$ for Cu, Ni, Sr, and V; $\pm 6-8\%$ for Ba, Cr, and Zr; and $\pm 10-25\%$ for Co, Sc, and Zn

^c (-) element not determined

^d country rock below sill

Mg #, when compared to the moderately zoned pyroxenes above the OZ. Average augites within the OZ are distinctly more Mg-rich (Mg # = 0.81; where Mg # = cation ratio Mg/(Mg + Fe)) than augite from above the OZ (Mg # = 0.75); however, average orthopyroxene is distinctly more Fe-rich within the OZ (En₇₁) as compared to above the OZ (En₇₆). The concentration of Cr₂O₃ in augite displays no statistically significant trends; however average Cr₂O₃ for augite within the OZ is higher (0.8%) than above the OZ (0.3%). The concentration of Cr₂O₃ in magnetite increases by a factor of 1.5 to 2 at the 25 m and 50 m

levels, but the four-fold increases that were previously reported by Shirley (1987) were not observed in this study. As noted by Shirley (1987), the large intrasample compositional variation resulting from moderate zoning in the pyroxenes makes correlations between mineral Mg# with bulk rock Mg# extremely difficult. Attempts to correlate the Cr₂O₃ of augite and magnetite with whole-rock Cr are also hampered by intrasample variability and the analytical limitations of the electron microprobe technique.

Compositional data for olivine (Fo) from both the Fort Lee and Alpine sections are plotted versus

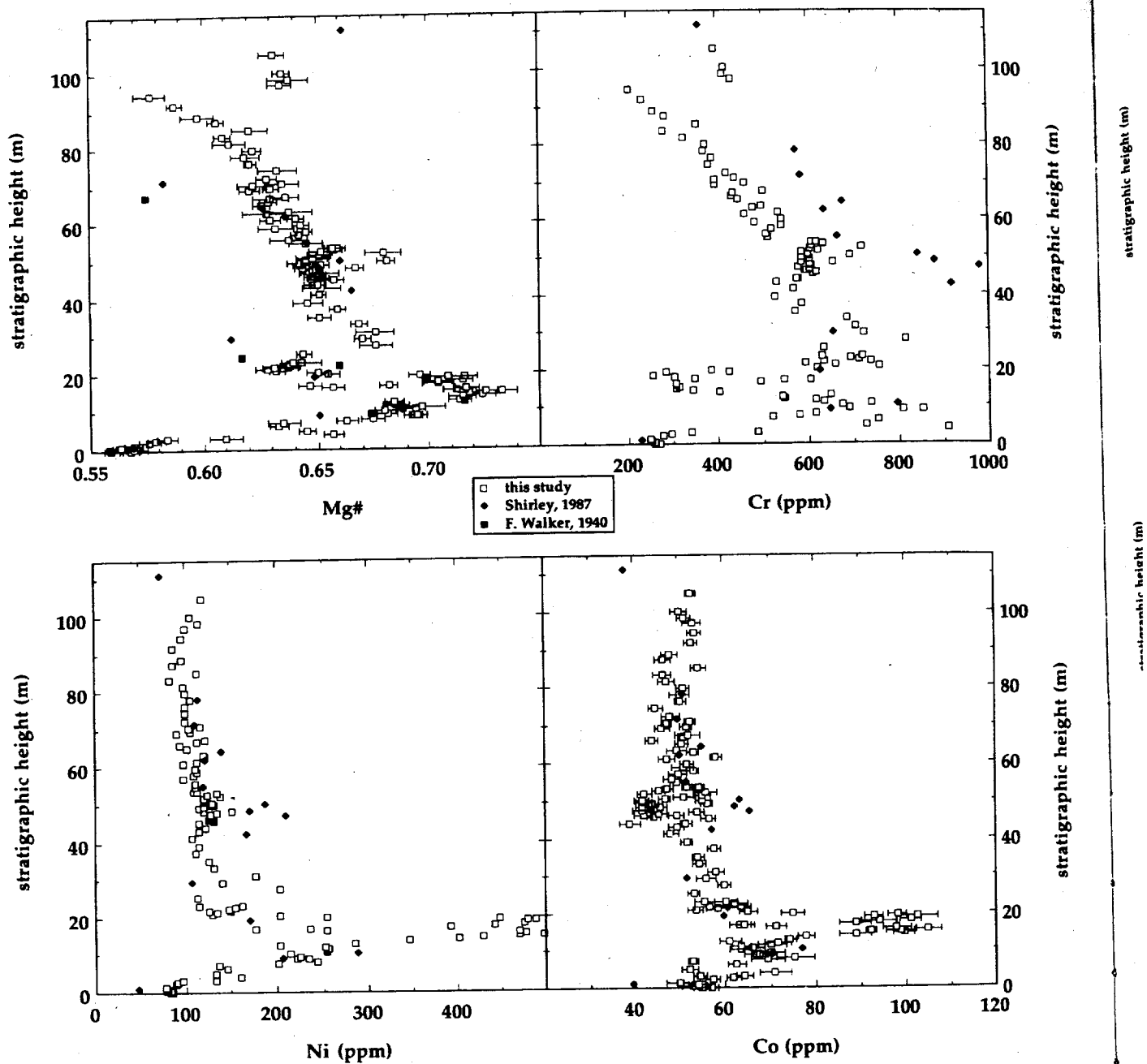


Fig. 5 Whole-rock data versus stratigraphic height (m) for the Mg#, Cr, Ni, and Co from the Fort Lee section. Data from this study (open squares), Walker (1940) (filled squares), and Shirley (1987) (filled diamonds). Error bars on Mg# and Co plots, and symbol size on Cr and Ni plots, represent the 95% confidence interval (2σ).

stratigraphic height in Fig. 7. Olivine is generally unzoned and no compositional difference related to grain size was identified, contrary to earlier reports (Walker 1940; Walker 1969). Samples from both localities contain large (0.6–0.8 mm diameter) and small (0.1–0.3 mm diameter) olivine grains that are of similar

average composition (Fig. 7). Olivine was found to be the most Mg-rich in the center of the OZ and progressively more Fe-rich near the upper and lower contacts, similar to observations reported by Walker (1969). At Fort Lee, the Fo content of olivine gradually increases from the 5 m (Fo_{57}) level until reaching maxima at the 15 m (Fo_{70}) and 19 m (Fo_{67}) levels, with a local minimum at 17 m (Fo_{63}). Similar compositional trends for olivine occur at Alpine; except for slightly more Fe-rich olivine (Fo_{57}) near the upper contact. The composition of olivine from the chilled margin at Fort Lee was found to be highly variable (Fo_{68} – Fo_{78}), in contrast to Walker's (1969) reported range (Fo_{79} – $Fo_{81.5}$). The Fo content of olivine is positively correlated with the

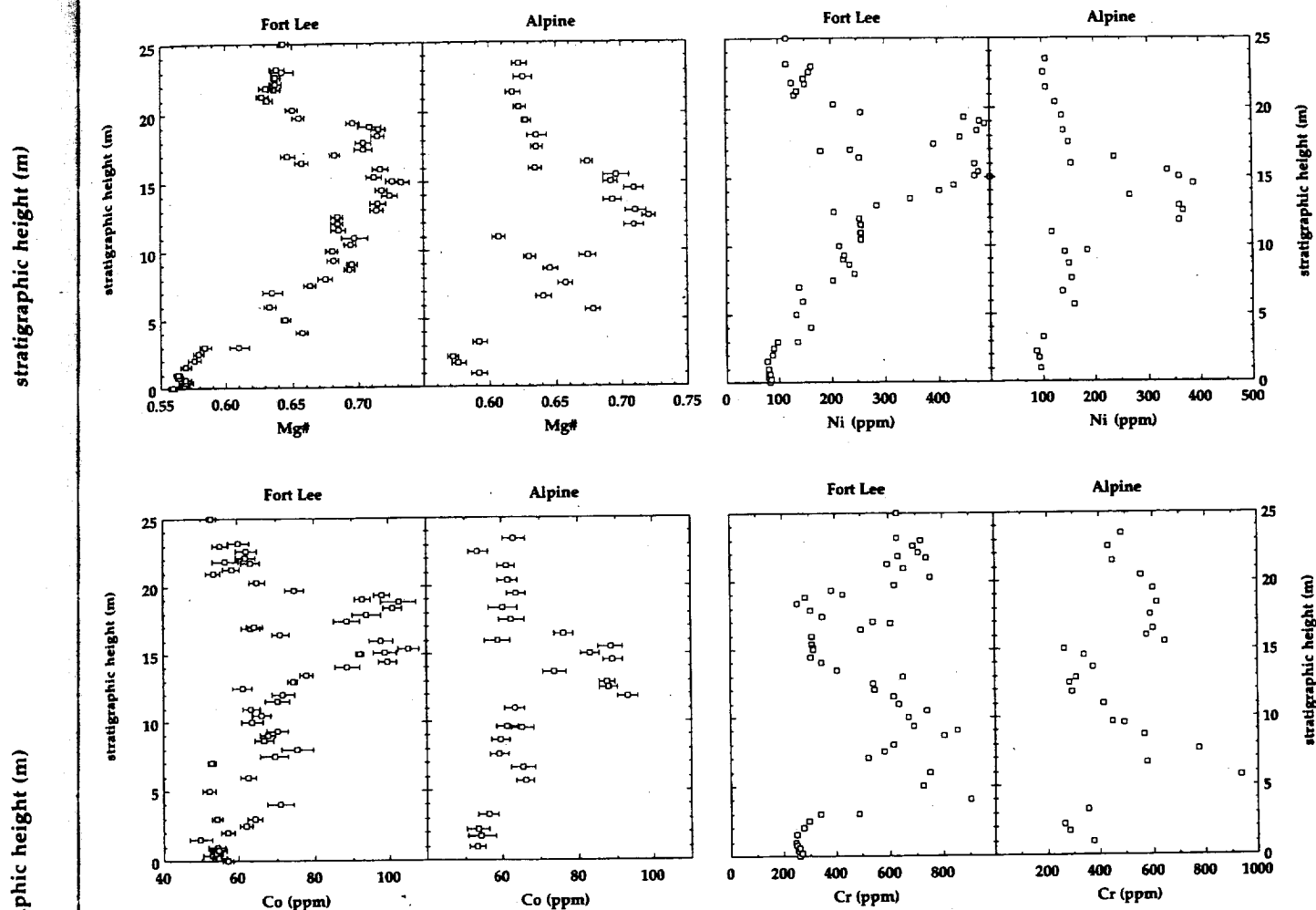


Fig. 6 Whole-rock data versus stratigraphic height (m) for the Mg#, Cr, Ni, and Co from the Fort Lee and Alpine sections. Error bars on Mg# and Co plots, and symbol size on Cr and Ni plots, represent the 95% confidence interval (2σ).

modal abundance of olivine and negatively correlated with the amount of trapped liquid (whole-rock K_2O content) suggesting that the olivine in the OZ may have reequilibrated with interstitial, Fe-rich trapped liquid (Naslund 1984; Barnes 1986; Conrad and Naslund 1989; Chalokwu and Grant 1990)

Pearce element ratios

A Pearce element ratio diagram of F'/K (where $F' = 0.5*(Fe + Mg) + 2*Ca + 3*Na$) vs Si/K can be used to examine intersample compositional variations in the Palisades sill (Fig. 8A). On such a plot, the fractionation of olivine, augite, or plagioclase will cause a linear trend with a slope of 1.0, the fractionation of orthopyroxene will cause a linear trend with a slope of 0.5, and the fractionation of Fe-oxides will cause a li-

near trend with a slope of ∞ (the plot assumes an augite of composition $Ca_{0.67}(Fe, Mg)_{1.33}Si_2O_6$; an augite richer in the Ca component would result in a slightly higher slope). Almost all of the samples from the lower part of the sill lie on the positive side of the chilled margin composition on a line with a slope of 0.87 suggesting that they represent mixtures of the initial liquid with cumulus plagioclase, and/or augite, and/or olivine, and orthopyroxene, similar to the conclusions of Steiner et al. (1992). Although the rocks are diabasic in texture, they are compositionally cumulates. Samples from the OZ lie on the same trend as the bulk of the sill, while samples from the anomalous horizons at 27 m and 45 m lie off the main trend at an average slope of 0.76 suggesting that they contain a higher proportion of cumulus orthopyroxene.

A plot of F''/K (where $F'' = Al + Fe + Mg - 2*Ca - Na$) vs Si/K can be used to separate the effects of olivine fractionation from augite and plagioclase (Fig. 8B). On such a plot, the fractionation of olivine will cause a linear trend with a slope of 2.0, the fractionation of orthopyroxene will cause a linear trend with a slope of 1.0, and the fractionation of augite or plagioclase will

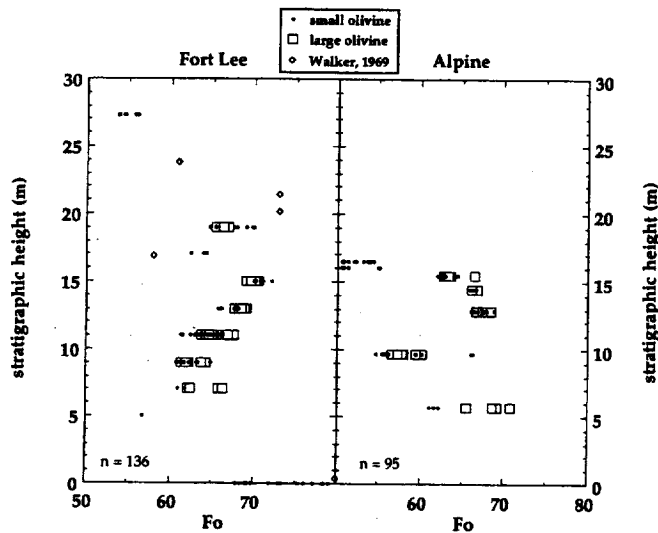


Fig. 7 Fo content in olivine versus stratigraphic height (m) from the Fort Lee and Alpine sections. Data from this study are core analyses of small grains (< 200 μ m diameter = filled circles) and large grains (400–800 μ m diameter = open squares). Total number of grains (n) analyzed for each location are given. Electron microprobe data from Walker (1969) are also shown (open diamond).

cause a linear trend with a slope of 0. The majority of samples from the Palisades sill plot on a linear trend with a slope of 0.23 indicating that they are dominated by cumulus plagioclase and augite with lesser amounts of cumulus orthopyroxene. Some of the scatter in the trend for samples not associated with the anomalous horizons results from the fact that the average slope decreases with increasing stratigraphic height reflecting the decrease in orthopyroxene abundance observed in thin section. The samples from the horizons at 27 m and 45 m again plot to the orthopyroxene side of the main trend with a slope of 0.32. The samples from the OZ plot over a wide area above the main trend suggesting that they have accumulated olivine. The wide scatter in these samples, however, indicates that the proportion of olivine to plagioclase + augite is quite variable, and suggests that the cumulus minerals in these samples have been mechanically sorted and do not represent crystallization of olivine "in situ" (Steiner et al. 1992). The relatively straight line and low slope trend for the majority of the Palisades samples, suggests that they can be derived from the chilled margin composition without the addition or subtraction of appreciable amounts of olivine. Pearce (1970) and Husch (1990) have also suggested that fractionation of early olivine is not necessary to generate the overall differentiation trend, based on whole-rock variation diagrams and mass-balance calculations. Steiner et al. (1992) suggest that early fractionation of olivine is not required by the major elements, but is required to account for trends in trace metals, especially Ni.

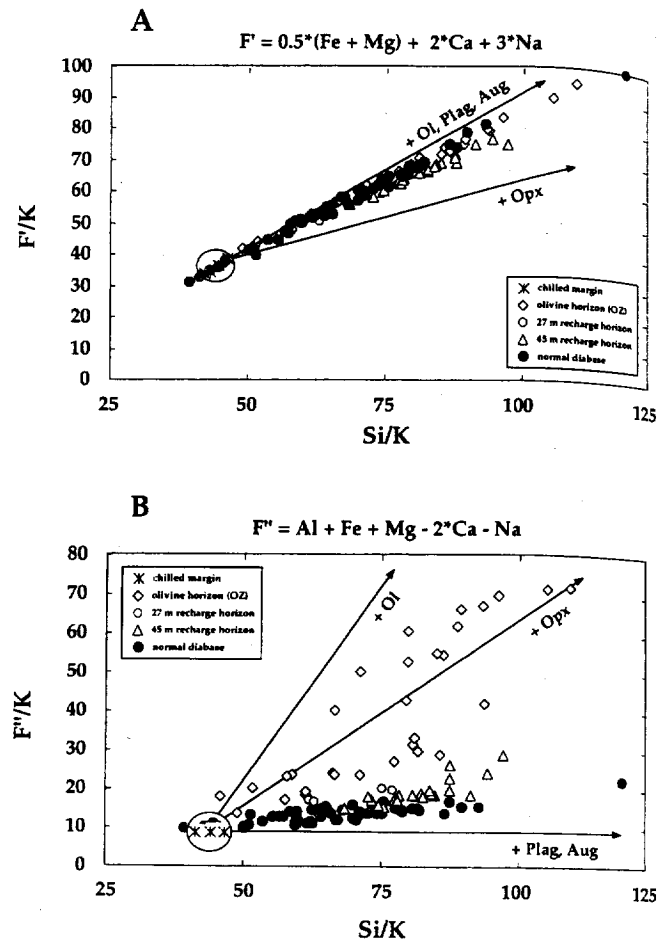


Fig. 8A Pearce Element Plot of F'/K versus Si/K where $F' = 0.5*(Fe + Mg) + 2*Ca + 3*Na$ for the Fort Lee, NJ section. Symbols represent normal diabase samples not associated with geochemical anomalies (filled circles), chilled margin samples (asterisks, circled), and also the geochemically anomalous horizons at the OZ (open diamonds), 27 m level (open circles), and 45 m level (open triangles). B Pearce Element Plot of F''/K versus Si/K where $F'' = Al + Fe + Mg - 2*Ca - Na$ for the Fort Lee, NJ section. Fractionation trends for olivine (Ol), plagioclase (Plag), augite (Aug), and orthopyroxene (Opx) are indicated by arrows.

Discussion

The olivine zone (OZ)

The nature of the upper and lower contacts of the OZ have been interpreted as sharp by Walker (1969), Shirley (1987), and Husch (1990) contrary to Walker (1940), who interpreted them as gradational. At Fort Lee, the petrographic and geochemical data indicate that the OZ has a gradational lower contact, a sharp upper contact, and a complex internal structure (Figs. 4, 6). This can be generalized to other locations along the strike of the sill; however, in detail, some localities (i.e. Alpine and Weehawken) have relatively sharp lower and upper contacts (Fig. 4B). At nearly all locations the upper contact of the OZ is distinctly sharper than is the

lower contact (Fig. 4B), and therefore, may be described as having a gradational lower contact and a sharp upper contact (cf. Bailey 1936). The general modal abundances of olivine in the OZ were reproduced by Gray and Crain (1969) with a quantitative model of simple gravity settling; however, gravity settling observed in natural settings typically produces modal and geochemical profiles with gradational lower and gradational upper contacts (Marsh 1989; Husch 1990). Fluid dynamical models (Komar 1972; Huppert and Sparks 1980; Kerr and Tait 1985) suggest that magma chamber recharge and/or flow differentiation could produce the modal and geochemical profiles observed in the OZ. The formation of the OZ may involve a combination of magma-chamber recharge, flow differentiation, gravity settling, and crystal sorting processes (Husch 1990; Steiner et al. 1992).

Time-scale calculations

Critical calculations of the time-scales involved in the formation of the OZ include: (1) the settling velocity of average-sized olivine crystals, (2) the time needed to fill the total volume of the Palisades sill, and (3) the time required for solidification of the OZ. The general Stoke's Law equation can be used to calculate the average settling velocity of spherical olivine crystals. The viscosity of the Palisades initial magma at a temperature of 1175° C with a H₂O content of 0.5% (Puffer 1992) can be estimated (Shaw 1972; Geist et al. 1985) to be approximately 425 poise. If we assume an olivine crystal of radius 0.1 mm (the average for olivine from the central part of the OZ at Fort Lee), an olivine density of 3.09 (corresponding to Fo₇₀ at 1175° C), and magma density of 2.68, the average settling velocity for olivine is 6.6 m/year. Calculations made using the composition of average ENA-OLN magma (Puffer 1992) and the parameters used above, yields a viscosity of 96 poise, a magma density of 2.76, and settling velocities on the order of 24 m/year. These settling velocities are similar to those calculated by Moore and Evans (1967) for olivine in the prehistoric Makaopuhi lava lake (i.e. 17 m/year).

Volume calculations are approximate because the sub-surface dimensions and the volume of material lost to erosion are not well constrained. If the shape of the Palisades sill was originally a circular (or elliptical) disc, with an average radius of 40 km and a thickness of 0.3 km, then its volume would be approximately 1500 km³. If the average radius is 75 km (Lewis 1907; Husch 1990), the volume is closer to 5000 km³. Hess (1956) speculated that emplacement of magma into the Palisades sill chamber was a "rapid, one-stage event" based on the constancy of chemical and petrographic characteristics of the chilled margin along the length of the sill. Puffer and Student (1992) and Philpotts (1992) also suggest high eruption rates to explain the morpho-

logy and volumes of extrusive basalt flows within the Newark and Hartford Basins. The largest historical eruption rate (0.02 km³ per day per km) documented is the 1783 Lakagigar (Laki) fissure eruption in Iceland (Thorarinsson 1969); however, eruption rates as large as 1 km³ per day per km have been proposed for the Yakima basalt on the Columbia River Plateau (Swanson et al. 1975). If the emplacement rate was between 0.01 and 0.1 km³ per day per km of fissure length, then the time required to fill the Palisades magma chamber with 1500 km³ of magma from a single 40 km long fissure would have been between 1 and 10 years.

Thermal models with general applications for the solidification of sheets and sills have been developed by Jaeger (1957) and Irvine (1970). Depending on the particular thermal model chosen, the time necessary for effective solidification of the olivine horizon ranges between 2 and 15 years (Gorring 1992). Irvine (1970) concluded that crystal fractionation processes tend to speed solidification by maintaining relatively steep temperature gradients across the roof contact, and therefore, Irvine's models yield considerably shorter times for solidification than do the models of Jaeger (1957). A combination of Irvine's (1970) "bottom crystallization" and "upper border zone" models is considered the most appropriate because the sill displays an asymmetric roof and floor sequence (Walker 1940; Walker 1969; Shirley 1987), and heat loss through the floor would be expected during the initial stages of cooling. This thermal model yields a solidification time of approximately 5 years for the OZ, and between 700 and 1000 years for the entire Palisades sill, similar to previous estimates (Shirley 1987).

These time-scale calculations suggest two important implications for the formation of the OZ: (1) gravity settling of olivine could only have occurred through a relatively small column (< 35 m) of HTQ magma before the solidification front passed through the 20 m level, and therefore, gravity settling at the scale envisioned by Walker (1969) and earlier workers probably did not occur, and (2) effective solidification of the OZ and emplacement of magma into the Palisades chamber probably occurred on similar time-scales, suggesting that the OZ may have formed during the initial emplacement process.

Emplacement of a heterogeneous initial magma

Estimated rates for the generation of magma in the mantle (Swanson 1972; Oxburgh 1980; Shaw 1980) suggest that the time necessary to generate 1500 to 5000 km³ of magma is probably greater than 10,000 years. The emplacement of the Palisades magma within a relatively short period of time suggests that it may have been collected and stored in a crustal, sub-Palisades magma chamber prior to emplacement (Walker 1969). Such a large volume of magma collecting at

in the OZ
horizon
horizon
be

125

where
ction.
with
(aste-
at the
(open
where
ction.
(Aug),

125

OZ
Shir-
(40),
the
the
oper
, 6).
the
(i.e.
wer
the
the

depth is unlikely to remain homogeneous, but rather is more likely to become density stratified. Many of the physical and petrologic characteristics of the OZ are consistent with the emplacement of magma from a stratified, sub-Palisades storage chamber within the upper crust. Stratification within this storage chamber would be characterized by a light, relatively crystal-free HTQ magma overlying a dense, olivine-normative magma (OZ magma) possibly charged with olivine phenocrysts. The storage chamber could be tapped such that the HTQ magma was initially emplaced into the shallow-level Palisades sill chamber, followed by a relatively small volume of OZ magma. Initial emplacement of the HTQ magma followed by rapid cooling would produce the chilled margins and a 5–10 m thick crystal-liquid mush zone (Marsh 1988) at the bottom of the sill. As the emplacement process continued in the Palisades chamber, the OZ magma would eventually be tapped and intruded into the largely molten HTQ magma. Rheological differences between the HTQ magma and the OZ magma would be sufficient to prevent appreciable mixing, but instead allow the OZ magma to spread laterally as finger-like projections (Pollard et al. 1975; Husch 1990) at an equilibrium density-level and to pond directly over the developing HTQ crystal-liquid mush zone, 5–10 m above the base of the sill. This explains the stratigraphic position and the along-strike variations in thickness of the OZ (Husch, 1990), and possibly the presence of flow banding (Walker 1969) in the internal contact at Kings Bluff. Convective mixing, driven by gravitational instability between light interstitial liquid within the HTQ mush zone and the overlying, dense OZ magma (Huppert and Sparks 1980; Kerr and Tait 1985) would produce a gradational lower contact for the OZ. Interaction and mixing between interstitial HTQ liquid and OZ magma might explain the systematic reequilibration of olivine to more Fe-rich compositions observed in the lower sections of the OZ. Mixing between REE-enriched, interstitial HTQ liquid and OZ magma could account for the similar REE abundances in the OZ and the chilled margin (Husch 1990, 1992). Local gravity settling of olivine crystals on the scale of a few meters could explain the abundance of large olivine grains in the lower sections of the OZ. This model also predicts a sharp upper contact for the OZ since the upper interface between the OZ magma and the overlying HTQ magma would have been dynamically stable with respect to density.

Some specific petrologic details of the OZ are more difficult to explain. The poikilitic texture, larger grain sizes, and the lack of strong zoning patterns of pyroxenes within the OZ suggests slower crystallization rates compared to rocks above and below the OZ (Walker 1969). Differences in crystallization rates could result from the emplacement of a slightly cooler OZ magma into a slightly hotter HTQ magma. A lower temperature for Walker's (1969) Pulse 2 was hy-

pothesized to explain the difference in Fo content of olivine between the chilled margin and the OZ. Alternatively, The OZ magma may have contained fewer pyroxene and plagioclase crystal nuclei, so that the poikilitic texture formed as a result of different nucleation densities not different cooling rates. The complex internal structure of the OZ may have formed in response to: (1) a second injection of OZ magma, (2) an internal crystal sorting process (Steiner et al. 1992), or (3) an interfingering phenomena during emplacement (Pollard et al. 1975; Husch 1990).

Magma chamber recharge

Geochemical anomalies at the 27 m and 45 m levels in the Palisades sill are interpreted as magma chamber recharge horizons; thus, following emplacement and formation of the OZ, the Palisades chamber experienced at least two additional magma pulses. Anomalies are indicated by abrupt geochemical reversals in Mg#, Ni, and Cr, abrupt decreases in grain size, and increases in modal orthopyroxene; and are consistent with the injection of a small-volume of hot, primitive magma into a cool, partially-differentiated magma present within the Palisades chamber. Elevated whole-rock Mg#, Cr, and Ni values persist over thicknesses of 6 to 10 m, which may represent the amount of dense, hybrid magma formed by mixing during recharge. The mixing of a primitive and a differentiated magma along a curved cotectic (a surface of multiple saturation in plagioclase, orthopyroxene, and augite) will result in a hybrid magma that is oversaturated in orthopyroxene if, as in most experimental systems, the cotectic surface is concave towards orthopyroxene. This effect is similar to that in which the mixing of differentiated and primitive magma saturated in chromite results in a hybrid magma oversaturated in chromite (Irvine 1977). Alternatively, the recharge horizons may be enriched in orthopyroxene because the incoming recharge magma was orthopyroxene-phyric. Contamination from the wall rocks of small feeder dikes could result in elevated silica activity (Philpotts and Asher 1993) and cause the precipitation of orthopyroxene. The sharp decrease in grain size near the 45 m level is consistent with a model in which a low-volume, hot magma would rapidly lose heat to a cooler, larger-volume, differentiated magma. Heat transfer between two magmas is likely to be much more efficient than transfer between magma and solid rock, because in the former case the cooler magma is able to carry heat away from the interface by convection (Huppert and Sparks 1980).

The sharp reversal in the differentiation trend at the 95 m level correlates with a previously described reversal in the Mg# between 78–111 m that has been attributed to magma chamber recharge (Shirley 1987). Field evidence; however, suggests that the reversal at the 95 m level is the result of a repetition of the strati-

graphi
fault is
evident
found
this le
abrupt
basal
This c
paral
east,
docu
Bluff.
graph
with
is no

Concl

In su
m o
to h
emp
ber
tion
cou
ma
for
rog
age
rap
(Sh
yez
ize
fro
(19
m
se
th
re
or
tc
th
of
o
n
r
c
p
t
t
i
l
(

graphic sequence by normal faulting. The proposed fault is never exposed in outcrop; however, convincing evidence for stratigraphic offset of the basal contact is found 1 km to the south, in Edgewater, New Jersey. At this location, the cliff exposure of the Palisades sill is abruptly displaced 300–400 m to the west, and the basal contact is displaced upward approximately 60 m. This discrepancy is consistent with a normal fault that parallels the strike of the sill and dips steeply to the east, analogous to the geometry of normal faulting documented by Walker (1969, p. 16, Fig. 2) at Kings Bluff. The trace of the proposed fault follows a topographic low along Hudson Terrace Ave. and coincides with the only interval in the lower 100 m of the sill that is not exposed in the Fort Lee area.

Conclusions

In summary, geochemical trends within the lower 100 m of the Palisades sill at Fort Lee, New Jersey appear to have been complicated by several factors including: emplacement of heterogeneous magma, magma chamber recharge, and normal faulting. Detailed compositional data from Fort Lee and Alpine, New Jersey coupled with estimates for the time-scales of critical magmatic processes suggest that the OZ may have formed as a result of the initial emplacement of a heterogeneous magma from a stratified, sub-Palisades storage chamber. Alternatively, if emplacement was very rapid, the OZ could represent a discrete recharge event (Shirley 1987; Husch 1990) that occurred shortly (< 5 years) after initial emplacement. The anomalous horizons at 27 m and 45 m are interpreted to have resulted from magma chamber recharge, following Shirleys (1987) interpretations; while the sharp reversal at 95 m appears to represent repetition of the stratigraphic sequence by normal faulting. Overall the lower part of the Palisades sill is composed of cumulate rocks that represent mixtures of early formed plagioclase, augite, orthopyroxene, and olivine with trapped liquid, similar to the model proposed by Steiner et al. (1992). Within the recharge horizons at 27 m and 45 m the proportion of orthopyroxene increased abruptly, either as a result of mixing between differentiated and primitive HTQ magma along a curved phase boundary or because the recharge magma was orthopyroxene-phyric. The OZ contains cumulus plagioclase, augite, and orthopyroxene in proportions similar to those in the rest of the lower part of the sill, but contains variable proportions of cumulus olivine, suggesting a mechanical sorting process (i.e. flow differentiation, crystal sorting), as proposed earlier by Husch (1990) and Steiner et al. (1992).

Acknowledgements We want to thank David Wark (Rensselaer Polytechnic Institute) and William Blackburn (SUNY-Binghamton) for assisting with electron microprobe analyses, John Tacinelli for

his help in the collection of samples, and Jerry Del Tufo of the Port Authority of NY/NJ for logistical support. We also thank Anne Hull and David Tuttle for help with the preparation of this manuscript. Constructive comments by Jeffrey C. Steiner and an anonymous reviewer vastly improved the manuscript and are greatly appreciated. A part of this research was carried out by the first author as a M.A. thesis submitted to the Department of Geological Sciences at the State University of New York at Binghamton. This study was supported by NSF grant EAR90-04209 to H.R. Naslund.

References

- Bailey EB (1936) American gleanings. *Trans Geol Soc Glasgow* 20:1–16
- Barnes SJ (1986) The effect of trapped liquid crystallization on cumulus mineral compositions in layered intrusions. *Contrib Mineral Petrol* 93:524–531
- Chalokwu CI, Grant NK (1990) Petrology of the Partridge river intrusion, Duluth Complex, Minnesota: 1. Relationships between mineral compositions, density, and trapped liquid. *J Petrol* 31:265–293
- Conrad ME, Naslund HR (1989) Modally-graded rhythmic layering in the Skaergaard intrusion. *J Petrol* 30:1–19
- Darton NH (1890) The relations of the traps of the Newark system in the New Jersey region. *US Geol Surv Bull* 67:13–77
- Dunning GR, Hodych JP (1990) U/Pb zircon and baddeleyite ages for the Palisades and Gettysburg sills of the northeastern United States: implications for the age of the Triassic/Jurassic boundary. *Geology* 18:795–798
- Feigenson MD, Carr MJ (1985) Determination of major, trace, and rare-earth elements in rocks by DCP-AES. *Chem Geol* 51:19–27
- Froelich AJ, Gottfried D (1988) An overview of early Mesozoic intrusive rocks in the Culpepper Basin, Virginia and Maryland. *US Geol Surv Bull* 1776:151–165
- Geist DJ, Baker BH, McBirney AR (1985) GPP: a program package for creating and using geochemical data files. Univ of Oregon, Center for Volcanology, Eugene
- Gorring ML (1992) The petrology and geochemistry of the lower 105 m of the Palisades sill, New Jersey. MA thesis, SUNY Binghamton, New York
- Gorring ML, Naslund, HR (1991a) Geochemical and petrographic signatures of magma chamber recharge in the Palisades sill, NJ-NY. *EOS Trans Am Geophys Union* 72:315
- Gorring ML, Naslund HR (1991b) A detailed investigation of the olivine horizon within the Palisades sill, NJ-NY. *Geol Soc Am Abstr Prog* 23:5:A270
- Gray NH, Crain IK (1969) Crystal settling in sills – a model for crystal settling. *Can J Earth Sci* 6:1211–1216
- Hess HH (1956) The magnetic properties and differentiation of dolerite sills – a critical discussion. *Am J Sci* 254:433–451
- Huppert HE, Sparks RSJ (1980) The fluid dynamics of a basaltic magma chamber replenished by influx of hot, dense ultrabasic magma. *Contrib Mineral Petrol* 75:279–289
- Husch JM (1990) Palisades sill: origin of the olivine zone by separate magmatic injection rather than gravity settling. *Geology* 18:699–702
- Husch JM (1992) Geochemistry and petrogenesis of the early Jurassic diabase from the central Newark Basin of New Jersey and Pennsylvania. *Geol Soc Am Spec Pap* 268:169–192
- Irvine TN (1970) Heat transfer during solidification of layered intrusions. Part I. Sheets and sills. *Can J Earth Sci* 7:1031–1061
- Irvine TN (1977) Origin of chromite layers in the Muskox intrusion and other stratiform intrusions: a new interpretation. *Geology* 5:273–277
- Irvine TN (1980) Magmatic infiltration metasomatism, double-diffusive fractional crystallization, and adcumulus growth in the Muskox intrusion and other layered intrusions. In: Hargraves RB (ed) *Physics of magmatic processes*. Princeton University Press, New Jersey, pp 325–383

- Jaeger JC (1957) The temperature in the neighborhood of a cooling intrusive sheet. *Am J Sci* 255:306-318
- Kerr RC, Tait SR (1985) Convective exchange between pore fluid and overlying reservoir of denser fluid: a post-cumulus process in layered intrusions. *Earth Planet Sci Lett* 75:147-156
- Komar PD (1972) Mechanical interactions of phenocrysts and flow differentiation of igneous dikes and sills. *Geol Soc Am Bull* 83:973-988
- Lewis JV (1907) Structure and correlation of Newark trap rocks of New Jersey. *Geol Soc Am Bull* 18:195-210
- Lewis JV (1908) The Palisades diabase of New Jersey. *Am J Sci* 26:155-163
- Marsh BD (1988) Crystal capture, sorting, and retention in convecting magma. *Geol Soc Am Bull* 100:1720-1737
- Marsh BD (1989) Magma chambers. *Ann Rev Earth Planet Sci* 17:439-474
- Moore JG, Evans BW (1967) The role of olivine in the crystallization of the prehistoric Makaopuhi tholeiitic lava lake, Hawaii. *Contrib Mineral Petrol* 15:202-223
- Naslund HR (1984) Petrology of the upper border series of the Skaergaard intrusion. *J Petrol* 25:185-212
- Oxburgh ER (1980) Heat flow and magma genesis. In: Hargraves RB (ed) *Physics of magmatic processes*, Princeton University Press, Princeton, NJ pp 161-200
- Pearce TH (1970) Chemical variations in the Palisade sill. *J Petrol* 11:15-32
- Philpotts AR (1992) A model for emplacement of magma in the Mesozoic Hartford basin. *Geol Soc Am Spec Pap* 268:137-148
- Philpotts AR, Asher PM (1993) Wallrock melting and reaction effects along the Higganum Diabase Dike in Connecticut: contamination of a continental flood basalt feeder. *J Petrol* 34:1007-1028
- Pollard DD, Muller OH, Dockstader DR (1975) The form and growth of fingered sheet intrusions. *Geol Soc Am Bull* 86:351-363
- Puffer JH (1992) Eastern North American flood basalts in the context of the incipient breakup of Pangea. *Geol Soc Am Spec Pap* 268:95-118
- Puffer JH, Student JJ (1992) Volcanic structures, eruptive style, and post-eruptive deformation and chemical alteration of the Watchung flood basalts, New Jersey. *Geol Soc Am Spec Pap* 268:261-277
- Shaw HR (1972) Viscosities of magmatic silicate liquids: an empirical method of prediction. *Am J Sci* 272:870-893
- Shaw HR (1980) The fracture mechanisms of magma transport from the mantle to the surface. In: Hargraves RB (ed) *Physics of magmatic processes*, Princeton University Press, Princeton, NJ pp 201-264
- Shirley DN (1987) Differentiation and compaction in the Palisades sill, New Jersey. *J Petrol* 28:835-865
- Smith RC, Rose AN, Lanning RM (1975) Geology and geochemistry of Triassic diabase in Pennsylvania. *Geol Soc Am Bull* 86:943-955
- Steiner JC, Walker RJ, Warner RD, Olsen TR (1992) A cumulus-transport-deposition model for the differentiation of the Palisades sill. *Geol Soc Am Spec Pap* 268:193-218
- Swanson DA (1972) Magma supply rate at Kilauea volcano. *Science* 175:169-170
- Swanson DA, Wright TL, Helz RL (1975) Linear vent systems and estimated rates of magma production and eruption for the Yakima Basalt on the Columbia Plateau. *Am J Sci* 275:877-905
- Thorarinsson S (1969) The Lakagigar eruption of 1783. *Bull Volcanol* 33:910-929
- Van Der Plas L, Tobi AC (1965) A chart for judging the reliability of point counting results. *Am J Sci* 263:87-90
- Walker F (1940) The differentiation of the Palisades diabase, New Jersey. *Geol Soc Am Bull* 51:1059-1106
- Walker KR (1969) The Palisades sill, New Jersey: a re-investigation. *Geol Soc Am Spec Pap* 111
- Weigand PW, Ragland PC (1970) Geochemistry of Mesozoic dolerite dikes from eastern North America. *Contrib Mineral Petrol* 29:195-214
- Wilson AD (1960) The micro-determination of ferrous iron in silicate minerals by a volumetric and a colorimetric method. *Analyst* 85:823-827